Title
Quadratic model for reservoir management: Application to the Central Valley Project

Journal
Water Resources Research, 21(5)

ISSN
0043-1397

Authors
Mariño, Miguel A
Loaiciga, Hugo A

Publication Date
1985-05-01

DOI
10.1029/wr021i005p00631

Peer reviewed

WATER RESOURCES RESEARCH, VOL. 21, NO. 5, PAGES 631–641, MAY 1985

Quadratic Model for Reservoir Management: Application to the Central Valley Project

MIGUEL A. MARIÑO AND HUGO A. LOAICIGA

Department of Land, Air, and Water Resources and Department of Civil Engineering University of California, Davis

A quadratic optimization model is applied to a large-scale reservoir system to obtain operation schedules. The model has the minimum possible dimensionality, treats spillage and penstock releases as decision variables and takes advantage of system-dependent features to reduce the size of the decision space. An efficient and stable quadratic programming active set algorithm is used to solve for the optimal release policies. The stability and convergence of the solution algorithm are ensured by the factorization of the reduced Hessian matrix and the accurate computation of the Lagrange multipliers. The quadratic model is compared with a simplified linear model and it is found that optimal release schedules are robust to the choice of model, both yielding an increase of nearly 27% in the total annual energy production with respect to conventional operation procedures, although the quadratic model is more flexible and of general applicability. The adequate fulfillment of other system functions such as flood control and water supply is guaranteed via constraints on storage and spillage variables.

INTRODUCTION

This paper is devoted to the development and application of a reservoir optimization model that yields monthly release policies. It constitutes a generalization of the models developed in the work by *Mariño and Loaiciga* [this issue] and the generalization consists of (1) capability to handle nonlinear energy generation rates in the objective function (maximization of system annual energy generation); (2) inclusion of nonlinear constraints, in particular those related to restriction on the magnitude of spillway discharges; (3) modeling of spillage (a decision variable that introduces considerable augmentation in the decision space) as a nonlinear function of storage, subject to the hydraulic properties of reservoir spillways; (4) introduction of nonlinear net loss functions (evaporation plus seepage plus direct rainfall) to replace linear net loss functions; and (5) exploitation of the presence of relatively small reservoirs downstream of larger ones (regulating reservoirs) by performing a (matrix) partition of the mathematical structure of the model that reduces the dimensionality of the state (storage) space by the number of existing regulating reservoirs.

The presence of two sets of decision variables (penstock releases and spillages) implies that the decision space dimensionality exceeds that of the state (storage) space, a situation leading to substantial difficulties in nonlinear optimization problems. This paper develops a methodology that makes possible to solve for spillages and penstock releases and derive their corresponding storage sequence in a stable and efficient manner. Furthermore, it is shown that it is possible to compute the decision and state variables by solving two-stage problems which are of minimum dimensionality, resulting in the most efficient way (both from storage and computational standpoints) to derive penstock release, spillage, and storage policies for reservoir operation problems.

The overall philosophy of the optimization scheme rests on the certainty equivalence controller principle (CEC) discussed in the work by *Mariño and Loaiciga* [this issue], which implies the use of the model in a real-time fashion. In essence, at every beginning of period (e.g., month), a forecast of inflows is made by a suitable model. Those forecasts are then treated as deterministic inputs, and a multistage deterministic problem is solved for the remaining of the reservoir operation horizon. The computed release policy is followed for the current period. As inflow forecasts deviate from actual realizations, new (updated) forecasts are computed, and a revised future release policy is developed on the basis of the observed state (storage) of the system and updated forecasts.

The multistage deterministic problem is decomposed into a sequence of two-stage quadratic problems that are solved one at a time. The solution of the two-stage problems, which, in general, have an indefinite reduced (or projected) Hessian matrix, is implemented in a stable manner guaranteeing accurate computation of the optimal release policies via a generalized active set method for quadratic problems. The active set method factorizes the reduced Hessian matrix and the null space of the constraint set, resulting in an accurate and fast convergence to the solution of the two-stage problems. The decomposition of the multistage problem into a sequence of two-stage problems is done within the framework of the progressive optimality algorithm (POA) [*Howson and Sancho*, 1975; *Turgeon*, 1981], leading to low storage requirements in the multipurpose reservoir application discussed below.

Some remarks on the approach followed in this paper are of importance. (1) Inflow forecasts are computed by a multivariate autogressive (AR) model, whose coefficients are estimated via maximum likelihood [*Mariño and Loaiciga*, 1983]. A unique feature of the maximum likelihood parameter estimation is that it permits to perform statistical tests on the structure of the model, i.e., on the order of the AR model, on the time invariance of the model parameters, and on the independence between streamflow realizations at different sites. Application of the AR model for streamflow forecasting yielded forecasted values within $\pm 10\%$ of actual values for the rivers in the Northern California Central Valley Project (NCVP). Statistical tests showed that the AR model of order 1 was adequate and that the streamflows were crosscorrelated, justifying the use of a multivariate model. (2) The reservoir operation horizon consists of 12 months, corresponding to a water year (October 1 to September 30). (3) The optimization model, as applied to the NCVP, has as objective function the maximization of the energy generated during each year. Since

Paper number 5W0026.
0043-1397/85/005W-0026$05.00

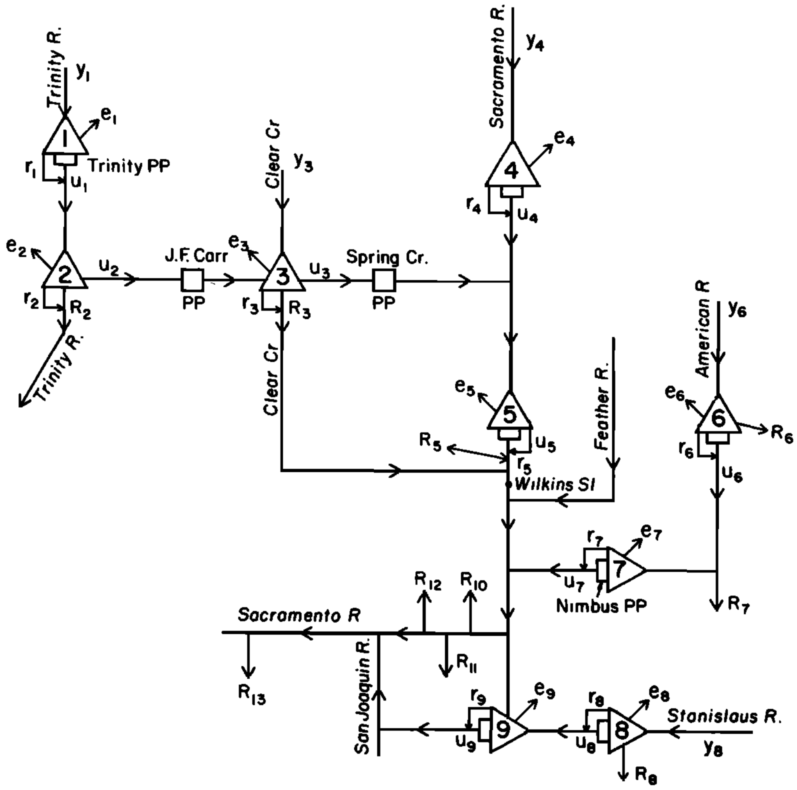

Fig. 1. Schematic representation of NCVP diversions (*R*), net losses (*e*), releases through penstocks (*u*), spills (*r*), and streamflows (*y*).

the NCVP power is sold as peaking capacity energy, there does not exist price differentials for different months, and hence maximizing total energy generation is equivalent to maximizing its dollar value. Also, the NCVP management aims at maximizing its cash revenues accruing from power sales while operating the system so as to provide adequate fulfillment of other functions by satisfying contractual agreements and specified ranges for storages and releases (e.g., for recreational or fisheries needs). Thus the multiple functions of the NCVP system are handled in the optimization model by obtaining a release schedule that maximizes energy revenues, while providing adequate service for other purposes via constraints on releases and storages. (4) The mathematical developments are in matrix notation. This notation is desirable to handle the multiunit nature of the NCVP and becomes essential in characterizing and solving the two-stage quadratic problems. The notation also is convenient for decoupling the system in order to reduce its dimensionality as shown below.

The objectives of this paper are (1) to develop all the numerical expressions to be used in the optimization model, following the general formulation of *Mariño and Loaiciga* [this issue], and to obtain, analyze, and compare the results with those obtained with a simpler linear model [*Mariño and Loaiciga*, this issue]; and (2) to describe an efficient algorithm to solve the sequence of two-stage quadratic problems, leading to the computation of spillage, penstock release, and storage policies of a multireservoir system (NCVP). The two-stage problems are solved in the most efficient way by an adequate reduction of their dimensionality.

SYSTEM AND PROBLEM DESCRIPTION

The system under analysis, the NCVP, is composed of the following reservoirs: (1) Clair Engle, (2) Lewiston, (3) Whiskeytown, (4) Shasta, (5) Keswick, (6) Folsom, (7) Natoma, (8) New Melones, and (9) Tullock. Figure 1 shows a schematic representation of the NCVP system and the points at which accretions and/or diversions occur. Adopting a 1-year planning horizon with monthly decisions, the following variables are defined

where

- $\mathbf{u}_t$ *n*-dimensional decision vector of penstock releases at the beginning of month *t*; its components are u_t^i, where *i* refers to the *i*th reservoir;
- $\mathbf{r}_t$ *n*-dimensional decision vector of spillages at the beginning of month *t*; its components are r_t^i;
- $\mathbf{x}_t$ *n*-dimensional state vector of storages at the beginning of month *t*; its components are x_t^i.

The time index *t* goes from $t = 1$ to $t = N + 1 = 13$, and *n* is the number of reservoirs in the system ($n = 9$ in the NCVP).

The continuity equation for the NCVP system for months *t* and $t + 1$ is

$$\mathbf{x}_{t+1} = \mathbf{x}_t + \Gamma_1 \mathbf{u}_t + \Gamma_2 \mathbf{r}_t + \mathbf{z}_t \tag{1}$$

in which Γ_1 and Γ_2 are lower triangular matrices that contain the topological arrangement of the system [*Mariño and Loaiciga*, this issue], and

$$\mathbf{z}_t = \mathbf{y}_t - \mathbf{e}_t - \mathbf{R}_t \tag{2}$$

where $\mathbf{y}_t$, $\mathbf{e}_t$, and $\mathbf{R}_t$ are the forecast inflow, net loss, and diversion vectors, respectively. There exist constraints on storages, penstock releases, spillages, and in the total release ($\mathbf{u}_t + \mathbf{r}_t$), which are discussed in the appendix.

The objective function is given by

$$\text{maximize} \sum_{t=1}^{12} E_t \tag{3}$$

where E_t is the total system power generation during month t, and for which an expression in terms of the variables $\mathbf{x}_t$, $\mathbf{u}_t$, and $\mathbf{r}_t$ will be developed. It is shown below that when posing (3) subject to the continuity equation (1) and other constraints as a sequence of two-stage problems, a quadratic programming (QP) two-stage problem must be solved at time t which is completely specified in terms of the storages only. The presence of spillage and releases implies the existence of more decision ($2n$) than state variables (n), which leads to complex numerical problems in any solution algorithm of the (nonlinear) optimization problem (e.g., in QP problems the Hessian matrix is singular), unless the decision space is appropriately reduced to be of size n. In this paper, such reduction is achieved via equality constraints on spillages as shown below. Upon solution of the optimization problem in terms of storages, spillages can be recovered from the equality constraints so that the system managers know how much of the total release is spillage and how much is penstock release. An important contribution of this paper is the development of an approach that permits to compute both optimal spillage and penstock releases simultaneously, and the introduction of a numerically stable algorithm for the solution of the two-stage problems, without which such a solution would not be possible.

ELEMENTS OF THE OPTIMIZATION MODEL

This section develops the necessary equations to arrive at the basic mathematical structure of the two-stage problems. Net losses, spillages, and energy equations are developed next.

Net Losses

Net losses consist of the net of evaporation, seepage, and direct rainfall. They are considered only for the major reservoirs (Clair Engle, Shasta, Folsom, and New Melones) because the smaller (constant storage or regulating) reservoirs have a small areal extent, and NCVP monthly operation records from 1960 to 1983 show that net losses are essentially zero. The following relations were developed from net loss data versus storages.

Clair Engle

$$e_t^1 = 3.33c_t^1 + 0.0078c_t^1\bar{x}_t^1 \tag{4}$$

Shasta

$$e_t^4 = 3.99c_t^4 + 0.0061c_t^4\bar{x}_t^4 \tag{5}$$

Folsom

$$e_t^6 = 2.67c_t^6 + 0.0094c_t^6\bar{x}_t^6 \tag{6}$$

New Melones

$$e_t^8 = 2.91c_t^8 + 0.0088c_t^8\bar{x}_t^8 \tag{7}$$

where in (4) e_t^1 denotes the net loss for month t in kilo acre foot (KAF); c_t^1 is a net loss coefficient [*Mariño and Loaiciga*, 1983] in feet per month, and $\bar{x}_t^1$ represents average storage during month t. The notation is similarly defined for (5)–(7).

Spillages

Spillway discharges are modeled by equations of the form

$$r_t^i = \bar{c}^i(h_t^i - d^i)\eta^i\delta^i \tag{8}$$

in which r_t^i is the discharge during month t at reservoir i (in kilo acre feet); $\bar{c}^i$ and η^i are coefficients determined from hydraulic properties of the ith spillway; h_t^i is (average) water surface elevation during month t at reservoir i (in feet); d^i is spillway crest elevation at reservoir i (in feet above mean sea level); and $\delta^i = 0$ when $h_t^i \le d^i$ and $\delta = 1$ when $h_t^i > d^i$. To develop spillway discharge equations, use was made of spillway discharge tables and curves, provided by the Central Valley Operations Office of the U.S. Bureau of Reclamation. Exponential interpolation of the spillway discharge tables and curves yielded the following equations (flows are in cubic feet per second (cfs) and elevations are in feet above mean sea level).

Trinity (at Clair Engle reservoir)

$$r_t^1 = 781(h_t^1 - 2370)^{1.29} \qquad r^2 = 98.4\% \tag{9}$$

in which r^2 is the adjusted regression correlation coefficient.

Lewiston

$$r_t^2 = 412(h_t^2 - 1871)^{0.626} \qquad r^2 = 99.8\% \tag{10}$$

Whiskeytown

$$r_t^3 = 992(h_t^3 - 1208)^{1.52} \qquad r^2 = 98.7\% \tag{11}$$

Shasta

$$r_t^4 = 314(h_t^4 - 1039)^{1.56} \qquad r^2 = 99.9\% \tag{12}$$

Keswick

$$r_t^5 = 720(h_t^5 - 547)^{0.436} \qquad r^2 = 99.2\% \tag{13}$$

Folsom

$$r_t^6 = 242(h_t^6 - 420)^{0.466} \qquad r^2 = 99.9\% \tag{14}$$

Nimbus

$$r_t^7 = 437(h_t^7 - 110)^{0.317} \qquad r^2 = 99.9\% \tag{15}$$

New Melones

$$r_t^8 = 420(h_t^8 - 1088)^{1.55} \qquad r^2 = 99.6\% \tag{16}$$

Tullock

$$r_t^9 = 750(h_t^9 - 495)^{0.478} \qquad r^2 = 95.0\% \tag{17}$$

Equations (9)–(17) need to be (1) converted from cubic feet per second to acre feet/month before they can be used in the development that follows and (2) expressed in terms of storage because the optimization is expressed in terms of storage rather than elevation as shown below.

Elevation versus storage data were analyzed to determine appropriate elevation-storage functions. The interval of interest is for the range of elevations above the spillway crest, otherwise the spillage would be zero, which means that only the shape of the elevation versus storage at high stages is of concern. Fortunately, from the perspective of numerical simplicity, the elevation-storage plots were nearly straight lines for all but low elevations. This behavior was determined to exist in the major reservoirs (Clair Engle, Shasta, Folsom, and New Melones) for which the elevation-storage curves were needed. A similar pattern holds for the smaller (regulating) reservoirs, but for those the interest is in a single elevation because the storage is held constant and there is no need for elevation-storage curves. The following linear functions were developed for the four major reservoirs (elevations h_t^i are in feet above mean sea level and storages x_t^i are in kilo acre feet):

Clair Engle

$$h_t^1 = 2142 + 0.0971 x_t^1 \qquad r^2 = 97.2\% \tag{18}$$

in which r^2 is the adjusted regression correlation coefficient.

Shasta

$$h_t^4 = 871 + 0.0444 x_t^4 \qquad r^2 = 99.3\% \tag{19}$$

Folsom

$$h_t^6 = 364 + 0.101 x_t^6 \qquad r^2 = 99.5\% \tag{20}$$

New Melones

$$h_t^8 = 860 + 0.0945 x_t^8 \qquad r^2 = 99.5\% \tag{21}$$

Elevations in feet above mean sea level corresponding to constant storages at Lewiston, Whiskeytown, Keswick, Natoma, and Tullock ($x_t^2 = 14.7$, $x_t^3 = 241$, $x_t^5 = 23.8$, $x_t^7 = 8.8$, and $x_t^9 = 57.0$ KAF, respectively) are 1901.1, 1210.0, 587.4, 125.1, and 501.6 feet, respectively. Upon substitution of the elevation-storage equations for the larger reservoirs and of the fixed elevations for the smaller (regulating) reservoirs into (9)–(17), and after a subsequent first-order Taylor expansion, the expression for spillage at the ith reservoir ($i = 1, 4, 6, 8$) becomes

$$r_t^1 \cong \hat{c}_t^i + \hat{d}_t^i x_t^i \tag{22}$$

in which the coefficients $\hat{c}_t^i$ and $\hat{d}_t^i$ have rather long algebraic expressions and will not be written out to conserve space. Both $\hat{c}_t^i$ and $\hat{d}_t^i$ depend on an initial guess of the storage value x_t^i about which the Taylor expansion was made. This first guess is automatically taken care of by the POA (see below), requiring a repeated solution of each two-stage QP problem as explained below. Notice also that spillway discharge functions for the regulating reservoirs (equations (10), (11), (13), (15), and (17)) need not be linearized because storage in those reservoirs is constant. The constancy of storage in the regulating reservoirs follows from their relative small size and has been observed in practice and in the results of a linear optimization model applied by *Mariño and Loaiciga* [this issue]. In (22), only the beginning of period x_t^i is shown; however, the spillage equations are actually based on average storage for period t, $\bar{x}_t^i = (x_t^i + x_{t+1}^i)/2$. Since in the two-stage QP problems of the POA the ending storage x_{t+1}^i is fixed [*Howson and Sancho*, 1975], it is a known quantity which is part of the expressions for $\hat{c}_t^i$ and $\hat{d}_t^i$ in (22). Equation (22) plays a fundamental role in the optimization model for it reduces the dimensionality of the decision space by linking spillages to storages and provides the required relation to recover spillage values upon solution for the x_t^i.

The previously developed equations for net losses and spillages (equations (4)–(7), (10), (11), (13), (15), (17), and (22) for $i = 1, 4, 6, 8$) are substituted into the continuity equation (1). Before doing this substitution, (1) is partitioned into vector components containing variables related to the major reservoirs ($i = 1, 4, 6, 8$) and those related to the regulating reservoirs ($i = 2, 3, 5, 7, 9$). For example, $\mathbf{x}_t^T = (\mathbf{x}_t^{(1)T} : \mathbf{x}_t^{(2)T}) = (x_t^1, x_t^4, x_t^6, x_t^8 : x_t^2, x_t^3, x_t^5, x_t^7, x_t^9)$. Similar partitions hold for $\mathbf{u}_t$, $\mathbf{r}_t$, and $\mathbf{z}_t$ in (1). Clearly, the matrices Γ_1 and Γ_2 in (1) need to be reordered conformally to maintain the appropriate link between the different vector components. It can be shown that Γ_1 and Γ_2 remain lower triangular matrices after the vector reordering (this reduces in approximately one half the number of computations in the solution algorithm). The reordered continuity equation (1) becomes (letting $\mathbf{x}_t^{(2)} = \hat{\mathbf{k}}$, to denote constant storages):

$$\begin{bmatrix} \mathbf{x}_{t+1}^{(1)} \\ \hat{\mathbf{k}} \end{bmatrix} = \begin{bmatrix} \mathbf{x}_t^{(1)} \\ \hat{\mathbf{k}} \end{bmatrix} + \begin{bmatrix} \Gamma_{11}^1 & 0 \\ \Gamma_{21}^1 & \Gamma_{22}^1 \end{bmatrix} \begin{bmatrix} \mathbf{u}_t^{(1)} \\ \mathbf{u}_t^{(2)} \end{bmatrix} + \begin{bmatrix} \Gamma_{11}^2 & 0 \\ \Gamma_{21}^2 & \Gamma_{22}^2 \end{bmatrix} \begin{bmatrix} \mathbf{r}_t^{(1)} \\ \mathbf{r}_t^{(2)} \end{bmatrix} + \begin{bmatrix} \mathbf{z}_t^{(1)} \\ \mathbf{z}_t^{(2)} \end{bmatrix} \tag{23}$$

Equation (23) shows that since the releases are functions of storages, it is possible to solve for the penstock release vector $\mathbf{u}_t$ in (23) in terms of an unknown vector $\mathbf{x}_t^{(1)}$ whose dimensionality is equal to only the number of nonregulating reservoirs, i.e., equal to four in the NCVP, since $\mathbf{x}_{t+1}^{(1)}$ is fixed in the POA and $\hat{\mathbf{k}}$ is known and constant. By substituting the loss and spillage equations into (23), and solving for $\mathbf{u}_t$, it can be shown that

$$\mathbf{u}_t = \begin{bmatrix} H_{11}^{t+1} & 0 \\ H_{21}^{t+1} & H_{22}^{t+1} \end{bmatrix} \begin{bmatrix} \mathbf{x}_{t+1}^{(1)} \\ \hat{\mathbf{k}} \end{bmatrix} - \begin{bmatrix} M_{11}^t & 0 \\ M_{21}^t & M_{22}^t \end{bmatrix} \begin{bmatrix} \mathbf{x}_t^{(1)} \\ \hat{\mathbf{k}} \end{bmatrix} - \begin{bmatrix} \mathbf{w}_t^{(1)} \\ \mathbf{w}_t^{(2)} \end{bmatrix} \tag{24}$$

in which matrices H_{ij}^{t+1} and M_{ij}^t ($i, j = 1, 2$) and vectors $\mathbf{w}_t^{(1)}$ and $\mathbf{w}_t^{(2)}$ follow from straightforward but lengthy algebraic operations performed on (23). A similar equation can be developed for $\mathbf{u}_{t-1}$ by analogous operation on the continuity equation for month $t - 1$. Equation (24) and a similar expression for $\mathbf{u}_{t-1}$, together with the energy equations to be developed next, are used to form the two-stage subproblems.

Energy Generation Rates

Mariño and Loaiciga [this issue] introduced a method to estimate the NCVP system energy production by developing energy production rate functions for each reservoir in megawatt hour per kilo acre foot (MWh/KAF). The energy produced in MWh during period t at reservoir i (E_t^i) is obtained by multiplying the energy generation rate (ξ_t^i, in MWh/KAF) by the penstock release (u_t^i, in KAF). It was found that for J. F. Carr power plant, Keswick, and Nimbus, linear functions are adequate, as is illustrated in Figure 2 for J. F. Carr power plant. The shape of the energy rates for other reservoirs indicated the suitability of a quadratic polynomial as shown in Figure 3, which depicts the energy rate as a function of storage for New Melones power plant. The following relations for the energy rates were obtained:

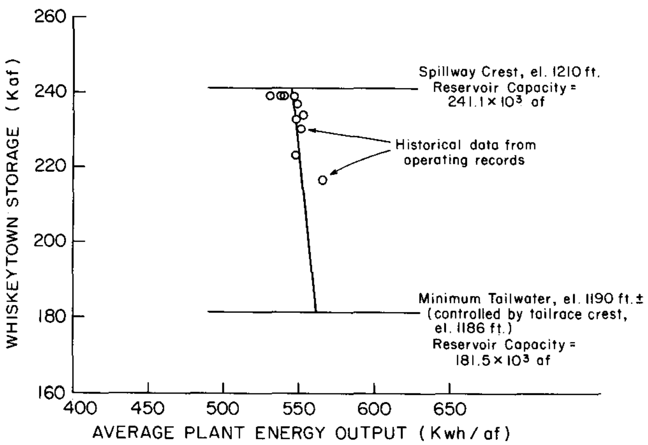

Fig. 2. J. F. Carr power plant gross generation curve.

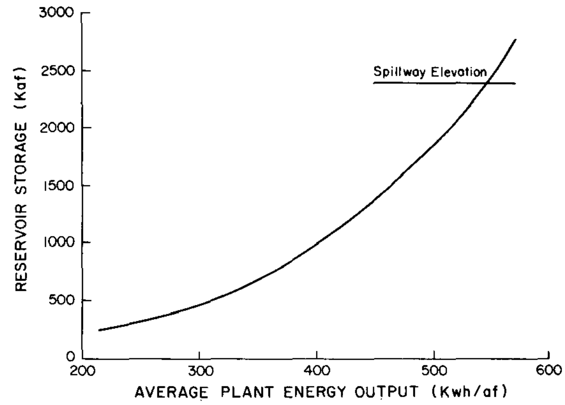

Fig. 3. New Melones power plant gross generation curve.

Trinity (at Clair Engle Lake)

$$\xi_t^1 = 133.0 + 0.228\bar{x}_t^1 - 0.468 \times 10^{-4}(\bar{x}_t^1)^2 \qquad r^2 = 99.3\% \tag{25}$$

Judge Francis Carr

$$\xi_t^2 = 606.3 - 0.254x_t^3 \qquad r^2 = 99.8\% \tag{26}$$

Spring Creek

$$\xi_t^3 = 445.0 + 0.738x_t^3 - 1.10 \times 10^{-3}(x_t^3)^2 \qquad r^2 = 99.8\% \tag{27}$$

Shasta

$$\xi_t^4 = 169.0 + 0.107\bar{x}_t^4 - 0.115 \times 10^{-4}(\bar{x}_t^4)^2 \qquad r^2 = 99.6\% \tag{28}$$

Keswick

$$\xi_t^5 = 80.3 + 0.6x_t^5 \qquad r^2 = 95.8\% \tag{29}$$

Folsom

$$\xi_t^6 = 171.0 + 0.265\bar{x}_t^6 - 0.130 \times 10^{-3}(\bar{x}_t^6)^2 \qquad r^2 = 98.7\% \tag{30}$$

Nimbus

$$\xi_t^7 = 26.3 + 0.80x_t^7 \qquad r^2 = 91.0\% \tag{31}$$

New Melones

$$\xi_t^8 = 169.0 + 0.275\bar{x}_t^8 - 0.479 \times 10^{-4}(\bar{x}_t^8)^2 \qquad r^2 = 98.6\% \tag{32}$$

Tullock

$$\xi_t^9 = 63.4 + 1.020x_t^9 - 1.37 \times 10^{-3}(x_t^9)^2 \qquad r^2 = 99.9\% \tag{33}$$

In (25), ξ_t^1 is the energy rate in MWh/KAF for Trinity power plant at Clair Engle Lake, $\bar{x}_t^1$ is the average reservoir storage in kilo acre feet during any month t, and r^2 is the adjusted regression correlation coefficient. Other terms in (26)–(33) are defined similarly. In (26) the energy rate depends on the storage of the downstream Whiskeytown reservoir. That stems from the fact that the storage at Lewiston is fixed and the energy gradient line from the intake of Clear Creek tunnel (connecting Lewiston and Whiskeytown reservoirs) to its discharging point (at Whiskeytown) is determined by the reservoir elevation at Whiskeytown (Figure 1). Due to the larger size of Whiskeytown as compared to Lewiston (241 and 14.7 KAF, respectively), it is likely that (slight) changes in elevations would occur at Whiskeytown and those changes would determine the differential head at J. F. Carr power plant and consequently its energy production rate. In fact, that is the case and it explains the negative slope in (26), which is consistent with Figure 2. Because Whiskeytown acts as a regulating reservoir, then for all practical purposes the storage at Whiskeytown (x_t^3) can be assumed fixed and equal in the average storage ($\bar{x}_t^3$). That is the reason for using x_t^3, rather than $\bar{x}_t^3$, in (26) and (27). Also, due to the regulating nature of Keswick, Lake Natoma (where Nimbus power plant is located), and Tullock, the (fixed) storages equal the average storages and thus the overbar has been omitted in (29), (31), and (33). It is clear that the approach followed herein handles a combination of linear and nonlinear energy rate functions. Notice that the storage at Lewiston has no role in the expression for energy rates (i.e., x_t^3 is used in equations (26) and (27)), yet it must be included in the continuity equation.

To set up the system energy production rate in matrix form, the quadratic energy rates are linearized. By performing a first-order Taylor series expansion about a guessed value for x_t^i, the energy generation rate becomes

$$\xi_t^i \simeq \hat{a}_t^i + \hat{b}_t^i x_t^i \qquad i = 1, 4, 6, 8 \tag{34}$$

in which the coefficients $\hat{a}_t^i$ and $\hat{b}_t^i$ depend on the initial guessed value for x_t^i (which is fixed, as was explained earlier while discussing the spillage equations), and whose lengthy expressions have been omitted due to space limitations. Clearly, no linearization is needed for linear energy rates, since the energy rate equations (e.g., equations (26), (29), and (31)) are already in the desired form given in (34).

The discussion on energy rates is completed by providing the vector-matrix expression of the energy rates for months t and $t - 1$ that are needed in the two-stage problems. Expressing the energy rates in forms similar to (34) for the entire NCVP system yields

$$\boldsymbol{\xi}_t = \begin{bmatrix} \hat{\mathbf{a}}_t^{*(1)} \\ \hat{\mathbf{a}}^{*(2)} \end{bmatrix} + \begin{bmatrix} B_{11}^{*t} & 0 \\ 0 & B_{22}^{*} \end{bmatrix} \begin{bmatrix} \mathbf{x}_t^{(1)} \\ \mathbf{k}^{*} \end{bmatrix} \tag{35}$$

in which

$$\hat{\mathbf{a}}_t^{*(1)T} = (\hat{a}_t^1, \hat{a}_t^4, \hat{a}_t^6, \hat{a}_t^8) \quad (36)$$

$$\hat{\mathbf{a}}^{*(2)T} = (\hat{a}^2, \hat{a}^3, \hat{a}^5, \hat{a}^7, \hat{a}^9) = (606.3, 445.0, 80.3, 26.3, 63.4) \quad (37)$$

$$B_{11}^{*t} = \text{diag}\,(\hat{b}_t^1, \hat{b}_t^4, \hat{b}_t^6, \hat{b}_t^8) \quad (38)$$

$$B_{22}^* = \text{diag}\,(-0.254, 0.738 - 1.10 \times 10^{-3}x_t^3, 0.60, 0.80, 1.020 - 1.37 \times 10^{-3}x_t^9) \quad (39)$$

$$\mathbf{k}^{*T} = (x_t^3, x_t^3, x_t^5, x_t^7, x_t^9) \quad (40)$$

The double appearance of superscript 3 in (40) follows from the use of x_t^3 in (26) and (27).

Solution of Two-Stage Problems

The objective function for the two-stage QP problems is readily available by using (24) to represent $\mathbf{u}_t$ and a similar expression (with the time index shifted by -1) for $\mathbf{u}_{t-1}$, i.e.,

$$\max E_t + E_{t-1} = \xi_t^T\mathbf{u}_t + \xi_{t-1}^T\mathbf{u}_{t-1} = k_t^* + \mathbf{q}_t^{*T}\mathbf{x}_t^{(1)} + \mathbf{x}_t^{(1)T}H_t^*\mathbf{x}_t^{(1)} \quad (41)$$

in which

$$\begin{aligned} k_t^* = {} & [\hat{\mathbf{a}}^{*(2)T} + \mathbf{k}^{*T}B_{22}^*] \\ & \cdot [H_{21}^{t+1}\mathbf{x}_{t+1}^{(1)} + H_{22}^{t+1}\hat{\mathbf{k}} - M_{22}^t\hat{\mathbf{k}} - \hat{\mathbf{w}}_t^{(2)} \\ & + H_{22}^t\hat{\mathbf{k}} - M_{21}^{t-1}\mathbf{x}_{t-1}^{(1)} - M_{22}^{t-1}\hat{\mathbf{k}} - \mathbf{w}_{t-1}^{(2)}] \\ & + [\hat{\mathbf{a}}_t^{*(1)T}(H_{11}^{t+1}\mathbf{x}_{t+1}^{(1)} - \hat{\mathbf{w}}_t^{(1)}) \\ & - \hat{\mathbf{a}}_{t-1}^{*(1)T}(M_{11}^{t-1}\mathbf{x}_{t-1}^{(1)} + \hat{\mathbf{w}}_{t-1}^{(1)})] \end{aligned} \quad (42)$$

$$\begin{aligned} \mathbf{q}_t^{*T} = {} & -\hat{\mathbf{a}}_t^{*(1)T}M_{11}^t - (\hat{\mathbf{a}}^{*(2)T} + \mathbf{k}^{*T}B_{22}^*)(M_{21}^t + H_{21}^t) \\ & + \mathbf{x}_{t+1}^{(1)T}(B_{11}^{*t}H_{11}^{t+1})^T - \hat{\mathbf{w}}_t^{(1)T}B_{11}^{*t} + \hat{\mathbf{a}}_{t-1}^{*(1)T}H_{11}^t \\ & - \mathbf{x}_{t-1}^{(1)T}(B_{11}^{*t-1}M_{11}^{t-1})^T - \mathbf{w}_{t-1}^{(1)T}B_{11}^{*t-1} \end{aligned} \quad (43)$$

$$H_t^* = B_{11}^{*t-1}H_{11}^t - B_{11}^{*t}M_{11}^t \quad (44)$$

where $\hat{\mathbf{a}}_t^{*(1)}$, $\hat{\mathbf{a}}^{*(2)}$, B_{11}^{*t}, B_{22}^*, and $\mathbf{k}^*$ have been defined in (36)–(40), and $\mathbf{x}_{t-1}^{(1)}$ and $\mathbf{x}_{t+1}^{(1)}$ are fixed in the two-stage problems. Notice that (41) is written in terms of $\mathbf{x}_t^{(1)}$ only, i.e., the solution to the two-stage problems is in terms of the nonregulating storage vector $\mathbf{x}_t^{(1)}$ only, of dimension four in this application. Had the formulation of the two-stage problems been expressed in terms of $\mathbf{x}_t$, $\mathbf{r}_t$, and $\mathbf{u}_t$, the total number of unknowns would have been 27 [*Mariño and Loaiciga*, this issue] for each two-stage QP problem.

The two-stage QP problem is fully specified by subjecting storages, penstock releases, spillages, and total releases to a set of (linear) constraints. As was stated in the introduction, constraints play two important roles in this study: (1) enforce feasibility due to physical and/or technical features in the system and (2) guarantee that functions other than power generation are adequately fulfilled, by introducing suitable constraints on penstock releases, spillages, and storages so as to satisfy contractual agreements and regulations related to flood control, wildlife and fisheries requirements, water quality, etc. *Mariño and Loaiciga* [1983] provided an extensive description of quantitative data on constraints imposed on the NCVP. It is clear that constraints on penstock releases and spillages can be expressed as constraints on storages by using (24) and the spillage equations (18)–(22), so that all the constraints can, in fact, be expressed in terms of $\mathbf{x}_t^{(1)}$. A qualitative description of the system constraints is contained in the appendix. Notice that the continuity equation is imbedded in (24) and has been substituted already in (41). Moreover, the development of the energy generation rates ξ_t^i, for all i, based on actual generation records, eliminates the need for nonlinear constraints on power production. From the general developments given for alternative linear and quadratic problems [*Mariño and Loaiciga*, this issue], it follows that the two-stage problems can be expressed as (dropping the constant term k_t^*)

$$\underset{\mathbf{x}_t^{(1)}}{\text{maximize}}\ F(\mathbf{x}_t) = \mathbf{q}_t^{*T}\mathbf{x}_t^{(1)} + \tfrac{1}{2}\,\mathbf{x}_t^{(1)T}H_t^{**}\mathbf{x}_t^{(1)} \quad (45)$$

subject to

$$A_t^*\mathbf{x}_t^{(1)} \le \mathbf{b}_t^* \quad (46)$$

in which the matrix of (linear) constraints A_t^* and the right-hand side vector $\mathbf{b}_t^*$ are mathematical expressions of the constraints listed in the appendix, and for convenience, $H_t^{**} = 2H_t^*$.

The sequential solution procedure to obtain monthly release schedules can be summarized as follows (for notational clarity, the superscript 1 on storages is dropped).

1. The initial and final states $\mathbf{x}_I$ and $\mathbf{x}_{13}$ are fixed. The subindex I can take values 1 through 11, depending on the month for which the future release policy is being computed. Forecast flows for the remaining 13-I months within the current water year and develop an initial feasible state trajectory $\{\mathbf{x}_t^{(k)}\}$, in which the time index is initialized at $t = I$, the counter k for the sweep iterations (from $t = I$ to $t = 12$) is set equal to 1, and the counter l for the iterations within each two-stage problem is set equal to zero.

2. Construct the QP problem given by (45)–(46), in which linearizations are made about $\mathbf{x}_t^{(l)}(\mathbf{x}_t^{(l)} = \mathbf{x}_t^{(k)}$ for $l = 0$ only).

3. Solve the QP problem and denote the solution by $\mathbf{x}_t^*$. If $\mathbf{x}_t^*$ does not satisfy a convergence test, then set $l = l + 1$, set $\mathbf{x}_t^{(l)} = \mathbf{x}_t^*$, and go to step 2. If $\mathbf{x}_t^* \cong \mathbf{x}_t^{(l)}$, set $k = k + 1$ and $\mathbf{x}_t^{(k)} = \mathbf{x}_t^*$, increase the time index by one, set $l = 0$, and go to step 2. Repeat steps 2 and 3 until a complete iteration sweep is performed ($t = I$ to $t = 12$). This ends the kth iteration.

4. Perform a convergence test for $t = I, I + 1, \cdots, 12$. If convergence is attained, go to step 5. Otherwise, set $k = k + 1$, $l = 0$, and go to step 2.

5. Apply the optimal computed policy for current month I. At the beginning of next month, set $I = I + 1$, and go to step 1.

A few remarks concerning the solution method are warranted. (1) In step 1, the fixed state $\mathbf{x}_I$ is specified. It is equal to the beginning of month storages for the nonregulating reservoirs. The final state $\mathbf{x}_{13}$ is also fixed. From previous operational experience, a value of $\mathbf{x}_{13}$ ranging from one half to two thirds of reservoir capacity was found to be appropriate (the value can be updated every month if deemed convenient). In this study a value of $\mathbf{x}_{13} = 7/12$ of reservoir capacity was adopted. (2) Initial policies are determined by a trial-and-error procedure that is based on past experience with NCVP operations [*Mariño and Loaiciga*, 1983]. (3) The bulk of the computations resides in step 3 of the solution procedure of the QP problem. In effect, the existence of an efficient, stable way to carry out step 3 practically implies the successful computation of the release policies.

The solution algorithm for the QP problems is briefly sketched next and consists of a generalized version of the active set method [*Fletcher*, 1981]. The generalization consists of making the algorithm capable of solving an indefinite QP problem (i.e., matrix H_t^{**} having negative and positive eigen-

TABLE 1. Optimal Release Policy, 1979–1980 (Policy 1)

	Clair Engle		Lewiston		Whiskeytown		Shasta		Keswick	
Month	Spill	Penstock	Spill	Penstock	Spill	Penstock	Spill	Penstock	Spill	Penstock
Oct.		99	26	73	5	77		300	50	327
Nov.		102	26	76	5	87		300	50	337
Dec.		89	26	63	5	76		664	50	690
Jan.		89	26	63	5	105		786	50	841
Feb.		89	26	63	5	168		786	110	844
Mar.		91	26	65	5	121	11	875	220	787
Apr.		92	26	66	5	93	78	394	50	515
May		209	26	183	5	192	56	495	50	693
June		209	26	183	5	190	14	436	50	590
July		209	26	183	5	186		680	50	816
Aug.		180	26	154	5	157		600	50	707
Sept.		100	26	74	5	78		353	50	381

	Folsom		Natoma		New Melones		Tullock		Delta Total
Month	Spill	Penstock	Spill	Penstock	Spill	Penstock	Spill	Penstock	Release
Oct.	20	170	19	168		157	55	102	721
Nov.		300	19	278		159	55	104	843
Dec.		300	19	278		199	110	89	1236
Jan.		476	184	289		218	110	108	1582
Feb.	70	406	184	289		213	110	103	1640
Mar.	156	344	184	313		205	110	95	1709
Apr.	45	305	62	285		217	110	107	1129
May	45	355	124	273		213	110	103	1353
June	23	277	33	264		211	110	101	1148
July	22	222	19	222		210	110	100	1317
Aug.	18	177	19	173		200	110	90	1149
Sept.	14	277	19	269		150	55	95	869

Releases are in kilo acre feet (1 KAF = 1.233×10^6 m^3). Total annual Delta releases = 14,697 KAF. Entries are the optimal implemented spillage and penstock releases at the beginning of each month. Total NCVP annual energy production corresponding to the optimal release policy = 7.764×10^6 MWh.

values), which is the case in this study. In particular, positive definite QP problems are automatically handled as a subcase. Other QP procedures such as complementary pivoting and Lemke's algorithm fail for indefinite problems. When solving a QP linearly constrained problem, at any iteration j of the active set method, a feasible point $\mathbf{x}^{(j)}$ with a corresponding matrix of active or binding constraints $A^{*(j)}$ and right-hand side $\mathbf{b}^{*(j)}$ are available. It is required to obtain a vector $\mathbf{p}^{(j)}$ such that $\mathbf{x}^{(j)} + \mathbf{p}^{(j)}$ is the minimum of $F(\mathbf{x})$ subject to the constraints $A^{*(j)}\mathbf{x}^{(j)} = \mathbf{b}^{*(j)}$ (notice that the subindex t is dropped also to ease the notation). Substitution of $\mathbf{x}^{(j)} + \mathbf{p}^{(j)}$ into (45) yields the following equality-constrained quadratic problem for $\mathbf{p}^{(j)}$,

$$\underset{\mathbf{p}^{(j)}}{\text{maximize}}\ \tfrac{1}{2}\,\mathbf{p}^{(j)T}\mathbf{H}^{**}\mathbf{p}^{(j)} + \mathbf{p}^{(j)T}(H^{**}\mathbf{x}^{(j)} + \mathbf{q}^*) \qquad (47)$$

subject to

$$A^{*(j)}\mathbf{p}^{(j)} = \mathbf{0} \qquad (48)$$

By virtue of (48), vector $\mathbf{p}^{(j)}$ can be written in terms of a basis of the null space of $A^{*(j)T}$, which is denoted by the matrix $Z^{(j)}$ [*Fletcher*, 1981], i.e., $\mathbf{p}^{(j)} = Z^{(j)}\mathbf{v}^{(j)}$, and then (47)–(48) can be written equivalently as the unconstrained problem

$$\underset{\mathbf{v}^{(j)}}{\text{maximize}}\ \{\tfrac{1}{2}\,\mathbf{v}^T(Z^{(j)T}H^{**}Z^{(j)})\mathbf{v} + \mathbf{v}^T Z^{(j)T}(H^{**}\mathbf{x}^{(j)} + \mathbf{q}^*)\} \qquad (49)$$

The solution $\mathbf{v}^{(j)}$ to (49) can be written as the solution to the equations

$$(Z^{(j)T}H^{**}Z^{(j)})\mathbf{v}^{(j)} = -Z^{(j)T}(H^{**}\mathbf{x}^{(j)} + \mathbf{q}^*) \qquad (50)$$

from which $\mathbf{p}^{(j)}$ of (47)–(48) is recovered by

$$\mathbf{p}^{(j)} = Z^{(j)}\mathbf{v}^{(j)} \qquad (51)$$

The vector $\mathbf{p}^{(j)}$ becomes a direction of search leading to a new iterate $\mathbf{x}^{(j+1)}$. In this study, problem (50) is solved by computing the LDL^T factors [*Stewart*, 1973] of the reduced Hessian matrix $Z^{(j)T}H^{**}Z^{(j)}$, which allows a check for the positive definiteness of $Z^{(j)T}H^{**}Z^{(j)}$, where L denotes a lower triangular matrix with unit diagonal elements, and D is a diagonal matrix. Further steps in the solution of the QP problem compute consecutive iterates $\mathbf{x}^{(1)}, \mathbf{x}^{(2)}, \cdots, \mathbf{x}^{(n)}$, where n is a finite integer, by using $\mathbf{x}^{(j+1)} = \mathbf{x}^{(j)} + \alpha\mathbf{p}^{(j)}$, where α is a step length determined by the geometry of the constraint step. Lagrange multipliers play an important role at each iteration because they determine the constraints that form the active set and whether the convergence to a solution is reached. To warrant accurate and stable estimates of Lagrange multipliers, their computation in this study has been accomplished by a stable QR factorization [*Stewart*, 1973] of the matrices $A^{*(j)T}$, as is proposed in the work by *Fletcher* [1981]. The initial $\mathbf{x}^{(1)}$, $A^{*(1)}$, and $\mathbf{b}^{*(1)}$ needed to start the active set iterations are computed by the method of *Fletcher* [1981]. It is important to use the factorizations LDL^T and QR named earlier. Otherwise, error propagation in the computations will lead to incorrect results in testing the convergence of the active set iterations and the positive definiteness of $Z^{(j)T}H^{**}Z^{(j)}$, which involve the eigenvalues of $Z^{(j)T}H^{**}Z^{(j)}$ and the values of the Lagrange multipliers, leading to a breakdown of the active set algorithm. Furthermore, the use of such factorizations allows

TABLE 2. Optimal Release Policy, 1979–1980 (Policy 2)

	Clair Engle		Lewiston		Whiskeytown		Shasta		Keswick	
Month	Spill	Penstock	Spill	Penstock	Spill	Penstock	Spill	Penstock	Spill	Penstock
Oct.		190	26	164	5	168		300	25	443
Nov.		190	26	164	5	175		338	50	463
Dec.		170	26	144	5	157		688	50	795
Jan.		100	26	74	5	116		728	50	794
Feb.		100	26	74	5	179		812	220	771
Mar.		100	26	74	5	130		876	220	786
Apr.		95	26	69	5	96	78	370	50	494
May		170	26	144	5	153	57	319	50	479
June		110	26	84	5	91	35	465	50	541
July		125	26	99	5	102		700	50	752
Aug.		109	26	84	5	87		602	25	664
Sept.		99	26	73	5	77		460	25	512

	Folsom		Natoma		New Melones		Tullock		Delta Total
Month	Spill	Penstock	Spill	Penstock	Spill	Penstock	Spill	Penstock	Release
Oct.	18	204	19	200		157	55	102	844
Nov.		290	19	268		159	55	104	959
Dec.		295	19	273		199	110	89	1336
Jan.		476	184	289		218	110	108	1535
Feb.	52	424	184	289		213	110	103	1677
Mar.	150	310	184	273		205	110	95	1668
Apr.	79	381	62	395		217	110	107	1218
May	45	275	125	192		213	110	103	1059
June	22	268	30	257		211	110	101	1089
July	22	278	19	278		210	110	100	1309
Aug.	19	161	19	158		200	110	90	1066
Sept.	15	238	19	231		150	55	95	937

Releases are in kilo acre feet (1 KAF = 1.233×10^6 m^3). Total annual Delta releases = 14,697 KAF. Entries are the optimal implemented spillage and penstock releases at the beginning of each month. Total NCVP annual energy production corresponding to the optimal release policy = 7.772×10^6 MWh.

us to update the factors L, D, Q, and R from one iteration to another rather than to compute them ab initio, resulting in substantial savings in the computations. Also, the triangularity of matrices $\Gamma_{11}{}^1$, $\Gamma_{11}{}^2$, $\Gamma_{22}{}^1$, and $\Gamma_{22}{}^2$ (see equation (23)) reduces the number of computations necessary to solve the two-stage problems (45)–(46) by approximately one half.

ANALYSIS OF RESULTS

By using the method outlined in the preceding section, release policies for the NCVP were computed for 1979–1980, a water year with average inflow conditions (total yearly inflow equaled 13,936 KAF). After deriving two initial release policies the model was run to determine if both policies yielded the same performance, as measured by the total annual system energy generated. Derivation of the initial policies (1 and 2) was accomplished by a trial-and-error procedure on the basis of past operation experience and with the assistance of the NCVP managing staff. Tables 1 and 2 show optimal releases corresponding to initial policies 1 and 2, respectively. These tables also show that substantial spillages occur in the regulating reservoirs (Lewiston, Keswick, Natoma, and Tullock; at Whiskeytown, spillages are slightly greater than the downstream water requirements of 3 KAF/month). The major reservoirs pass most of their total release through penstocks, with the exception of (high inflow) March. Optimal policies 1 and 2 in Tables 1 and 2 are clearly different except for the subsystem New Melones-Tullock where initial policies 1 and 2 yielded the same optimal release and state sequences (state or storage sequences have been omitted to conserve space). Both solutions 1 and 2 yielded the same volume of Delta releases as specified in Tables 1 and 2 (annual total Delta release = 14,697 KAF). The total annual energy production is almost the same for policies 1 and 2, 7.764×10^6 and 7.772×10^6 MWh, respectively. For all practical purposes, it can be claimed that the two alternative optimal policies produce a comparable performance as measured by energy production. Table 3 summarizes the results obtained from the linear model [*Mariño and Loaiciga*, this issue], the actual operations, and the quadratic model of this paper. The linear model results in larger Delta releases (14,773 KAF) than those obtained with the quadratic model (14,697 KAF, for both policies 1 and 2) and also in larger annual energy production (8.077×10^6 MWh as compared to 7.764×10^6 and 7.772×10^6 MWh for the two optimal policies of the quadratic model).

Figure 4 shows that the state trajectories at Shasta for the different models. It is evident that quadratic policies 1 and 2 follow a pattern similar to the linear policy but, overall, maintain a lower storage elevation. That is explained by the fact that when spillages are functions of storage, there is a penalty for achieving higher levels because the spilled (nonenergy producing) water increases exponentially with the differential of reservoir elevation minus spillway crest elevation. It can be expected that penstock releases will increase (in the quadratic model) to keep reservoir levels from reaching such high elevations. Because energy production is linear in the penstock release (recall that $E_t = \xi_t{}^T \mathbf{u}_t$), it would follow that the quadratic model is more likely to generate more energy than the linear model; however, it was stated earlier that the linear

TABLE 3. Actual and Maximized Energy Production for 1979–1980

Month	Trinity Power Plant at Clair Engle Actual	Linear	Quad. 1	Quad. 2	Judge Francis Carr Power Plant Actual	Linear	Quad. 1	Quad. 2	Spring Creek Power Plant Actual	Linear	Quad. 1	Quad. 2
Oct.	30.4	73.9	37.4	71.1	36.8	112.4	39.8	98.8	42.3	111.2	43.0	93.9
Nov.	9.6	71.2	39.4	68.9	4.8	112.4	43.1	98.8	19.5	115.2	49.7	97.8
Dec.	17.1	61.4	33.3	60.0	15.4	98.5	34.3	86.8	19.2	101.3	42.5	87.8
Jan.	6.2	29.7	33.8	35.6	···	41.9	34.3	44.6	23.9	95.5	58.7	64.8
Feb.	17.7	31.1	34.9	37.2	3.4	41.9	34.3	44.6	55.3	87.0	93.9	100.1
Mar.	73.4	32.2	36.3	38.2	78.2	41.9	35.4	44.6	99.5	50.0	67.6	72.7
Apr.	44.9	32.9	37.0	36.8	53.5	41.9	36.0	41.6	54.7	56.6	52.0	53.7
May	21.2	33.7	84.6	66.6	21.2	41.9	99.8	86.8	18.6	46.5	107.3	85.5
June	51.5	75.3	84.2	43.1	55.2	101.2	99.8	50.6	59.6	102.2	106.2	50.9
July	54.3	39.4	82.9	48.8	57.2	44.7	99.8	59.7	57.2	45.7	104.0	57.2
Aug.	75.7	37.6	69.6	41.9	87.2	42.9	84.0	50.6	85.9	44.0	87.8	48.1
Sept.	71.1	36.5	38.5	37.3	84.7	44.2	41.4	44.0	88.6	45.7	44.7	43.0
Total	473.1	555.1	611.8	585.7	497.6	765.9	681.9	751.4	623.3	901.0	857.5	855.2
E_a/E_m		0.58	0.77	0.81		0.65	0.73	0.66		0.69	0.73	0.73

Month	Shasta Power Plant Actual	Linear	Quad. 1	Quad. 2	Keswick Power Plant Actual	Linear	Quad. 1	Quad. 2	Folsom Power Plant Actual	Linear	Quad. 1	Quad. 2
Oct.	76.5	112.1	116.2	116.2	19.0	47.0	30.9	41.9	37.7	53.5	48.6	57.9
Nov.	89.6	126.2	116.2	130.7	20.7	51.3	32.1	43.8	41.3	77.9	80.1	76.3
Dec.	111.1	251.3	254.5	253.9	23.2	81.6	65.3	75.2	37.2	71.3	71.3	69.0
Jan.	237.4	266.9	302.5	279.2	47.6	81.6	79.5	75.1	107.0	118.4	127.2	126.0
Feb.	209.9	310.7	316.3	326.4	39.2	81.6	79.8	72.9	84.3	139.9	122.7	127.8
Mar.	228.3	323.7	358.3	358.3	49.9	81.6	74.4	74.3	130.0	147.2	104.8	94.7
Apr.	112.9	126.1	162.0	151.8	29.0	37.3	48.7	46.7	99.8	126.3	93.2	116.2
May	164.4	128.8	203.8	131.4	33.7	36.2	65.5	45.3	82.0	131.0	108.6	84.0
June	212.9	129.5	178.3	190.6	47.3	45.5	55.8	51.2	66.6	76.4	84.7	81.9
July	237.9	307.5	273.1	281.0	52.2	77.0	77.2	71.1	84.4	63.4	65.6	84.4
Aug.	165.7	310.2	232.8	232.2	43.6	81.6	66.9	62.7	35.6	93.5	53.3	48.1
Sept.	86.8	289.0	131.8	172.9	29.3	81.6	36.0	48.4	40.5	86.8	83.5	69.4
Total	1933.4	2682.2	2646.0	2625.6	434.7	784.5	712.2	708.7	846.4	1185.5	1045.5	1035.8
E_a/E_m		0.72	0.73	0.74		0.55	0.61	0.61		0.71	0.81	0.82

Values are in 10^3 MWh. Power plant was not in operation where no values are shown. E_a is actual energy production, E_m is maximized energy production. Quads 1 and 2 denote a quadratic model using initial policies 1 and 2, respectively.

TABLE 3. (Continued)

Month	Nimbus Power Plant at Lake Natoma Actual	Linear	Quad. 1	Quad. 2	New Melones Power Plant Actual	Linear	Quad. 1	Quad. 2
Oct.	4.6	6.4	5.6	6.7	···	71.6	75.0	75.0
Nov.	4.7	10.0	9.3	8.9	···	70.4	73.2	73.2
Dec.	4.7	10.0	9.3	9.1	···	68.1	87.6	87.6
Jan.	8.7	10.0	9.6	9.6	19.6	81.9	94.4	94.4
Feb.	6.7	10.0	9.6	9.6	23.6	92.1	94.1	94.1
Mar.	10.6	10.0	10.4	9.1	47.8	90.9	90.3	90.3
Apr.	9.7	7.7	9.5	13.2	55.8	90.4	92.1	92.1
May	9.1	8.2	9.1	6.4	39.5	85.8	87.5	87.5
June	7.6	7.8	8.8	8.6	23.3	84.4	84.6	84.6
July	9.7	6.5	7.4	9.3	38.5	80.9	79.1	79.1
Aug.	4.3	10.0	5.8	5.3	22.1	74.9	66.3	66.3
Sept.	4.6	10.0	9.0	7.7	9.0	64.8	41.7	41.7
Total	84.9	106.5	103.4	103.5	279.2	956.5	966.0	966.0
E_a/E_m		0.80	0.82	0.82		0.29	0.29	0.29

Values are 10^3 MWh. Power plant was not in operation where no values are shown. E_a is actual energy production, E_m is maximized energy production. Quads 1 and 2 denote a quadratic model using initial policies 1 and 2, respectively.

model resulted in a greater energy production level than the quadratic model. The resolution of the contradiction established by this argument and the observed results (which indicate more energy from the linear model) lies in the fact that energy production is a quadratic function of storages and that offsets the effect of the higher penstock release, for in the linear case the storages are greater. In the more realistic quadratic model, the trade-off between higher elevations and

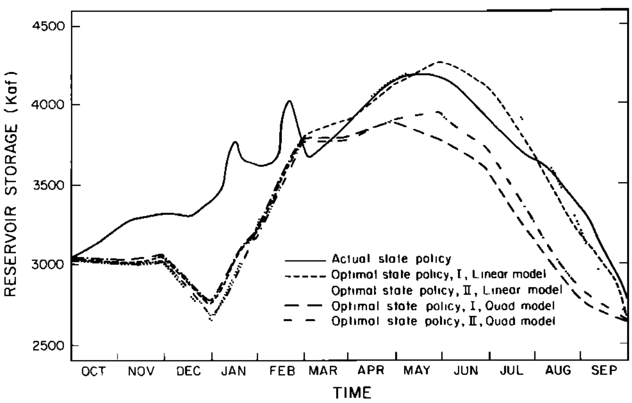

Fig. 4. Operation of Shasta reservoir, water year 1979–1980.

smaller releases is more complex than in the linear case [*Mariño and Loaiciga*, this issue]. It can be observed in Table 3 that values of E_a/E_m (actual over maximized annual energy ratios) are higher for the quadratic model than for the linear model. The overall E_a/E_m ratio for policy 1 of the quadratic model is $5.2/7.764 = 0.67$, slightly larger than the 0.64 obtained with the linear model [*Mariño and Loaiciga*, this issue], implying that a potential increase of up to 27% over energy actually produced could be achieved by using release policies from the quadratic model. A 27% increase will be about 1.4 $\times 10^6$ MWh per year with average inflow conditions.

The similar forms of the state trajectories shown in Figure 4 for the linear and quadratic models can be explained by noticing that high inflow forecasts result in a drawdown of reservoirs in December, mainly by routing large volumes of water through penstocks. Reservoir elevations are relatively steady throughout the winter so that the trade-off between elevation and discharge is optimal in the sense that for given conditions, the total energy would be maximized. The volume of water released during the summer (4,967 KAF in May to August), obtained from the quadratic model policy (Table 1), is larger than the agricultural requirements (2,698 KAF in May to August). This points to the feasibility of extending agricultural activities in the Sacramento-San Joaquin Valley. Finally, at the expense of a moderate increase in the complexity of the quadratic model, both in its formulation and solution, it appears that the quadratic model should be preferred over the linear model due to the closer representation to the actual system that it commands.

CONCLUSIONS

The application of the quadratic optimization model and its comparison with a linear model developed earlier by the authors lead to the following conclusions.

1. Both models lead to a potential increase in the annual energy generation, as was demonstrated for a water year of average streamflow conditions. The quadratic model implemented in this paper yielded a potential increase of 27% in the total annual energy production for the NCVP case study.

2. The quadratic model showed that the Sacramento-San Joaquin Valley agricultural water deliveries can be increased by adopting the optimal release policies. This suggests the possibility of expanding irrigated areas, providing better leaching of agricultural fields, and improving conjunctive management of surface and groundwater reservoirs.

3. Although the release policies computed by the quadratic and linear models were similar in this study, there are reasons for preferring the quadratic model. First, the quadratic model leads to problems of lower dimensionality (fewer decision variables) and provides a closer representation of the physical features of the system, particularly with regard to nonlinearities in the objective function and constraints. Second, because of its capability to incorporate spillages explicitly, the quadratic model can handle a reservoir system of more complicated configuration and complex mass balance (continuity) equation.

APPENDIX

The constraints considered in the two-stage problems (45)–(46) are as follows.

Constraints on total releases for month t,

$$\mathbf{u}_t + \mathbf{r}_t \leqq \mathbf{W}_t \tag{A1}$$

in which $\mathbf{W}_t$ is a maximum permissible total release vector.

Constraints on maximum penstock releases for month t,

$$\mathbf{u}_t \leqq \mathbf{U}_{t,\max} \tag{A2}$$

in which $\mathbf{U}_{t,\max}$ is maximum permissible penstock vector.

Constraints on minimum penstock releases for month t,

$$\mathbf{u}_t \geqq \mathbf{U}_{t,\min} \tag{A3}$$

where $\mathbf{U}_{t,\min}$ is minimum permissible penstock release vector.

Constraints on water requirements for month t and any demand point k,

$$\mathbf{c}_t^{kT}(\mathbf{u}_t + \mathbf{r}_t) \geqq D_t^k, \forall k \tag{A4}$$

where $\mathbf{c}_t^k$ is a vector representing a linear combination of total releases that add up to satisfy a minimum demand at control point k, D_t^k.

Constraints on spillages for month t,

$$\mathbf{r}_t \leqq \mathbf{R}_t \tag{A5}$$

in which $\mathbf{R}_t$ is a vector of maximum spillages.

Constraints on maximum and minimum storages for month t,

$$\mathbf{x}_t \leqq \mathbf{X}_{t,\max} \tag{A6}$$

$$\mathbf{x}_t \geqq \mathbf{X}_{t,\min} \tag{A7}$$

in which $\mathbf{X}_{t,\max}$ and $\mathbf{X}_{t,\min}$ are maximum and minimum permissible storage vectors.

In addition to constraints (A1)–(A7), there is an analogous set of constraints for month $t - 1$. Substitution of (23)–(24) into (A1)–(A7) and into the analogous constraints for month $t - 1$, and after some algebraic operations, yields the constraint matrix A_t^* and the right-hand side vector $\mathbf{b}_t^*$ in (46).

Acknowledgments. The research leading to this report was supported by the University of California, Water Resources Center, as part of Water Resources Center Project UCAL-WRC-W-634. We thank G. Link, of the Central Valley Operations Office, U.S. Bureau of Reclamation, Sacramento for his valuable assistance in providing data and explanations with regard to the operation of the California Central Valley Project.

REFERENCES

Fletcher, R., *Practical Methods of Optimization*, vol. 2, *Constrained Optimization*, John Wiley, New York, 1981.

Howson, H. R., and N. G. F. Sancho, A new algorithm for the solution of multi-stage dynamic programming problems, *Math. Program.*, *8*, 104–116, 1975.

Mariño, M. A., and H. A. Loaiciga, Optimization of reservoir operation, with applications to the Northern California Central Valley Project, *Water Sci. and Eng. Pap. 3013*, 444 pp., Dept. of Land, Air, and Water Resources, Univ. of Calif., Davis, 1983.

Mariño, M. A., and H. A. Loaiciga, Dynamic model for multireservoir operation, *Water Resour. Res.*, this issue.
Stewart, G. W., *Introduction to Matrix Computations*, Academic, New York, 1973.
Turgeon, A., Optimal short-term hydro scheduling from the principle of progressive optimality, *Water Resour. Res.*, *17*(3), 481–486, 1981.

H. A. Loaiciga and M. A. Mariño, Department of Land, Air, and Water Resources, University of California, Davis, CA 95616.

(Received March 12, 1984;
revised December 11, 1984;
accepted December 11, 1984.)